

A Density-Based Proteomics Sample Fractionation Technology: Folate Deficiency–Induced Oxidative Stress Response in Liver and Brain

Wenkui Lan,¹ Jayita Guhaniyogi,¹ Marc J. Horn,¹ Jun Q. Xia,² and Beverly Graham²

¹Prospect Biosystems, LLC, Newark, NJ; ²Pel-Freez Biologicals, Inc., Rogers, AR

Folate deficiency (FD) alters hepatic methionine metabolism and is associated with increased hepatocellular apoptosis. Additionally, mice deprived of folate showed increased oxidative damage in brain tissue, leading to cognitive impairment. Most previous studies have focused independently on either liver, the main tissue of folate storage and metabolism, or brain, where folate regulates neurogenesis and programs cell death. The aim of this study was to apply a powerful, rapid proteomics approach to understand potential subcellular correlations of folate deficiency in both brain and liver of the same rat. This approach combined a new density-based sample fractionation technology (enhanced density gradient extraction = Edge technology) with other conventional proteomics techniques, such as western blot analysis, 2DE, and mass spectrometry. The brain and the liver from individual rats, fed normal or FD diets for 6 wks, were homogenized and then fractionated using the Edge 200 Separation System. Subsequently, all fractions from brain and liver, from control and treated rats, were analyzed by western blot using two markers of oxidative stress: glutathione peroxidase 1 (GPx1) and glucose-regulated protein 75 (GRP75). Certain fractions were selected based on western blot analysis and were further analyzed by 2DE. Protein spots of interest were identified by MALDI-TOF/TOF. The results demonstrated that Edge technology provides a powerful density based separation and enrichment method for rapid screening of potential FD markers and their possible correlations to both liver and brain diseases.

KEY WORDS: folate deficiency, oxidative stress, Edge technology, sample fractionation, subcellular fractionation, sample enrichment.

Folate is a cofactor in one-carbon metabolism, which is a series of biosynthetic pathways crucial for DNA synthesis, DNA repair, and various methylation reactions.¹ Folate cannot be synthesized biologically in humans and most of the mammals, and thus must be obtained from food and dietary supplements. Dietary folate is required for normal development, particularly for pregnant women and the elderly. Epidemiological and experimental studies have shown that folate deficiency is not only linked to neurodegenerative and psychological disorders, including stroke, Alzheimer's disease, Parkinson's disease, and depression,^{2–8} but also contributes to cancer and cardiovascular diseases.^{9–15} The most common explanation for folate deficiency promoting various dis-

eases is that it disturbs one-carbon metabolism, increasing the level of homocysteine, which is a cytotoxic amino acid that can induce gene and DNA strand breakage, as well as apoptosis.¹⁶

An increasing number of reports suggest that oxidative stress can be induced by folate deficiency, which will cascade DNA damage, alter one-carbon metabolism, and trigger multiple organ damage and neurodegenerative disorders.^{17,18,35–38} Also, oxidative stress and oxidative damage can alter protein functions in many ways, including directly modifying catalytic amino acids, changing critical amino acid residues in binding or regulatory sites, and altering proteolytic susceptibility and states of aggregation.^{19–21} However, most of these studies were focused on only a single organ, such as liver or brain.^{22–26} In animals, the liver is an important organ for folate storage and metabolism. Brain, on the other hand, is the most sophisticated and complex organ in the whole body. A previous study, however, has reported that long-term folate deficiency would alter folate concentration and

ADDRESS CORRESPONDENCE AND REPRINT REQUESTS TO: Wenkui Lan, Ph.D., Prospect BioSystems, LLC, 211 Warren Street, Newark, NJ 07103 (phone: 973-242-6500 ext 102; fax: 973-215-2558; email: wlan@prospectbiosys.com).

distribution differentially in rat tissues.³⁵ Today, little is known about folate deficiency–induced oxidative stress at the subcellular level in a single tissue. Furthermore, there are no reports about the potential subcellular correlation of folate deficiency in multiple tissues in the same animal. In addition, more data are still required to clearly explain the cellular and molecular mechanisms connecting folate deficiency and various diseases.

Recently, advanced proteomics technologies have become valuable tools to better understand the normal biology and physiology of cells, microorganisms, tissues and organs.^{27–33} Proteomic approaches might help to close the gap between traditional pathologic, physiologic, and genomic studies, as well as to help understand the mechanisms of various diseases caused by folate deficiency. Today, there are only a few reports using proteomics to study folate deficiency and folate-related diseases.^{34,20,21} In this study, we report a powerful, rapid proteomics method, which combines a newly developed density-based sample fractionation technology (enhanced density gradient extraction—Edge technology) with other conventional proteomics techniques such as western blot analysis, 2DE, and mass spectrometry. The aim of this study is to apply this proteomic approach to understand potential subcellular correlations of folate deficiency in both brain and liver in the same rat. Furthermore, this methodology will help to rapidly identify some unique proteins and potential biomarkers for better understanding, diagnosis, and treatment of various diseases associated with folate deficiency.

MATERIALS AND METHODS

Animals, diets, and tissue collection. Eight healthy male Sprague-Dawley rats, 7–8 wks old, approximately 150–175 g each, were used. Rats were housed four per cage in a temperature-controlled room with a 12-h light/dark cycle and given access to water and food *ad libitum* at all times. The Dyets version of the Clifford/Koury folate-deficient L-amino acid rodent diet with 1% succinyl sulfathiazole (Cat. No. 517777, Dyets, Inc., Bethlehem, PA) was used as folate deficiency (FD) diet, and the Dyets L-amino acid-defined rat diet (Cat. No. 517804) was used as control diet. Two groups of four rats were fed with control diet for 2 wks. Then one group of rats were fed continually with the control diet and the other group of rats were changed to FD diet. After a 4-wk feeding and growing period, the rats were starved overnight. The starved rats were anesthetized and dissected. Their brains and livers were collected and perfused with phosphate-buffered saline (PBS) and snap frozen in liquid nitrogen. Each harvested organ was wrapped separately and stored at -80°C for future analysis. All rats were handled humanely and maintained in facilities with accreditation by the Association for the

Assessment and Accreditation of Laboratory Animal Care and Use Committee. All the studies were in accordance with the guideline of the Care and Use of Laboratory Animals of the National Research Council, 1996.

Chemicals. HEPES, EDTA, sodium chloride, tris (2-carboxyethyl) phosphine hydrochloride, tris (2-carboxyethyl) phosphine, urea, thiourea, CHAPS, SDS, sucrose, acetonitrile (ACN), and ammonium bicarbonate were purchased from J.T. Baker (Phillipsburg, NJ); Tween-20, and potassium chloride from EMD Chemicals (Gibbstown, NJ); methanol from VWR (West Chester, PA); trichloroacetic acid (TCA), trifluoroacetic acid (TFA), acetone, tri-butylphosphine, iodoacetamide, α -cyano-4-hydroxy-cinnamic acid, protease inhibitor cocktail, and C7 detergent from Sigma-Aldrich (St. Louis, MO); trypsin from Promega (Madison, WI); and bromophenol blue, ampholyte, and Biosafe Coomassie Blue from Bio-Rad (Hercules, CA).

Homogenization. The entire homogenization process was performed on ice. One frozen liver or brain was thawed in ice-cold 1X homogenization buffer (20 mM HEPES, 10 mM KCl, 1 mM Na_2EDTA , and 250 mM sucrose, pH 7.4, for liver; 20 mM HEPES, 1 mM Na_2EDTA , and 320 mM sucrose, pH 7.4, for brain) with protease inhibitor cocktail. The tissue was dissected into 2- to 3-mm³ pieces, and the liquid was carefully discarded. The tissue pieces were resuspended in five volumes of homogenization buffer, and the suspension was transferred to a glass homogenizer. Using a loose pestle, the tissue was homogenized up-down 10 times, and then using a tight pestle, the tissue was homogenized up-down 10 times. The homogenate was transferred to centrifuge tubes and centrifuged at 1000 g for 10 min to remove nuclei. The supernatant, which is post-nuclear supernatant (PNS), was kept on ice for further fractionation.

Density-based fractionation. A prototype of the Edge 200 Separation System from Prospect Biosystems, LLC (Newark, NJ) was used for the density-based fractionation. The fractionation procedure is described in the following steps: (1) Transfer 3 mL of PNS into a rotor sample container. (2) Insert the rotor sample container into a rotor, and spin at 95,000 rpm for 30 min. (3) Decelerate the rotor to rest and remove the supernatant. Almost all of the subcellular particles are pelleted on the vertical wall of the sample container. (4) Add 1 mL of homogenization buffer into the rotor sample container, and resuspend the pellet using a vortex. (5) Spin the rotor with the rotor sample container for 2 min at 95,000 rpm. (6) Decelerate the rotor and remove the supernatant. All potential soluble proteins adsorbed on the pellet in the previous step are washed off. (6) Added 0.5 mL of first density extraction medium (10% w/w sucrose, 20 mM HEPES, 10 mM KCl, pH 7.4) into the rotor sample container and

vortex to resuspend the pellet. (7) Spin the rotor with the sample container for 2 min at 95,000 rpm. (8) Decelerate the rotor and remove the supernatant to a clean microcentrifuge tube to give fraction 10%. (9) Add second density extraction medium (15% w/w sucrose, 20 mM HEPES, 10 mM KCl, pH 7.4) to the sample container and vortex to resuspend the pellet. (10) Repeat steps 7 and 8 to obtain fraction 15%. (11) Continue these same steps using serially increasing sucrose density extraction medium: 20%, 25%, 30%, 35%, 40%, 45%, 50%, 55%, and 60%. A total of 11 fractions are obtained.

Protein assay. Protein concentration of each fraction was measured using BCA Protein Assay kit or Bradford Protein Assay kit (Pierce, Rockford, IL) according to the manufacturer's protocol.

SDS-PAGE and western blot. Samples from all fractions were diluted 1:1 with Laemmli Sample Buffer (Bio-Rad) containing 5% v/v of 2-mercaptoethanol. Bio-Rad Criterion 26-well 4–20% Tris-HCl gels and Tris/glycine/SDS buffer were used for electrophoresis. Electrophoresis was performed first at a constant 110 V for 10 min and then at a constant 150 V until the dye front reached the end of the gel.

The Bio-Rad Trans-Blot transfer cell and 40% Tris/glycine, 40% Tris/glycine/SDS, 20% methanol were used to transfer proteins to Bio-Rad Immun-Blot PVDF membranes at a constant 20 V overnight. For glutathione peroxidase (GPx-1), a goat polyclonal antibody (Santa Cruz Biotechnology, Santa Cruz, CA), western blots were carried out at 1:500 dilution. For GRP 75, a goat polyclonal antibody (Santa Cruz Biotechnology), western blots were performed at 1:2000 dilution. Donkey anti-goat IgG-HRP (Santa Cruz Biotechnology) was used as secondary antibody for both GPx-1 and GRP 75. Peroxidase activities were detected by a chromogenic substrate using Pierce's Metal Enhanced DAB substrate. The stained membranes were scanned using Umax PowerLook 1100 (Dallas, TX). The digitized images were analyzed using ImageJ software (NIH, Bethesda, MD).

Sample preparation and two-dimensional gel electrophoresis. To each selected fraction, based on western blot analysis, one volume of COMS solution (40 mM Tris, 7 M urea, 2 M thiourea, and 1% C7 detergent) was added, and samples were reduced with tri-butylphosphine and alkylated with iodoacetamide. The reduced and alkylated samples were precipitated with TCA, followed by ice-cold acetone wash. The precipitated proteins were resuspended in isoelectric focusing (IEF) rehydration buffer (7 M urea, 2 M thiourea, and 2% CHAPS). The protein concentration of each fraction was determined using Bradford Protein assay kit prior to 2DE.

All 2DE were performed following a standard procedure with minor modification. Briefly, samples contain-

ing 200 µg of proteins were placed in rehydration trays, Bio-Rad linear-gradient immobilizing pH gradient (IPG) strips pH 5–8 were laid on top, and allowed to rehydrate overnight. IEF was performed on the Bio-Rad Pretean IEF unit following the manufacturer's suggested program, resulting in about 30,000 V-h of focusing time. After equilibration of IPG strips, Bio-Rad Criterion 4–20% IPG+1 Tris-HCl gels were used for the second dimension (SDS-PAGE) at a constant 110 V for 10 min and at a constant 150 V until the dye front reached the end of the gel. Gels were stained with BioSafe Coomassie Blue for 45 min and destained for 2 h using DI water. All fractions were run in duplicate. The stained gels were scanned using a Bio-Rad Molecular Imager GS-800 Calibrated Densitometer. The digitized images were analyzed and compared using PDQuest software (Bio-Rad).

In-gel digestion and MALDI mass spectrometry. Selected gel spots, based on image analysis, were excised and washed with 30% ACN in 50 mM ammonium bicarbonate, followed by proteolytic digestion using 25 ng/µL of trypsin for 2 h on a robotic platform (TECAN, Durham, NC). The resulting peptides were extracted with 30 µL of 1% TFA and mixed with 7 mg/mL α -cyano-4-hydroxy-cinnamic acid matrix in a 1:1 ratio. The mixture was spotted onto a matrix-assisted laser desorption/ionization (MALDI) plate. The peptides were analyzed on a 4700 Proteomics Analyzer tandem mass spectrometer (Applied Biosystems, Framingham, MA). Mass spectra (m/z 800–3,600) were acquired in positive ion reflector mode with internal mass calibration. The fifteen most intense ions were selected for subsequent MS/MS sequencing analysis in 1kV mode. Protein identification was performed by searching the combined MS and MS/MS spectra against the SwissProt database (V. 46) using a local MASCOT search engine (V. 1.9) on a GPS (V. 3.5, ABI) server. The following parameters were used: trypsin was selected as the protease; a maximum of one missed cleavage was allowed; carbamidomethyl (C) and oxidation (M) were selected as variable modification. Precursor mass tolerance was set at 50 ppm; MS/MS mass tolerance was set at 0.3 Da.

RESULTS AND DISCUSSION

Introduction of Edge Technology and Edge 200 Separation System

Edge technology is a newly developed non-denaturing front-end sample fractionation technology. It is a step-wise extraction of a particle mixture using extracting media of increasing densities. Edge technology provides a, powerful, well defined, and reproducible fractionation method for proteomics analysis. It is compatible with all downstream analyses, including gel electrophoresis, HPLC,

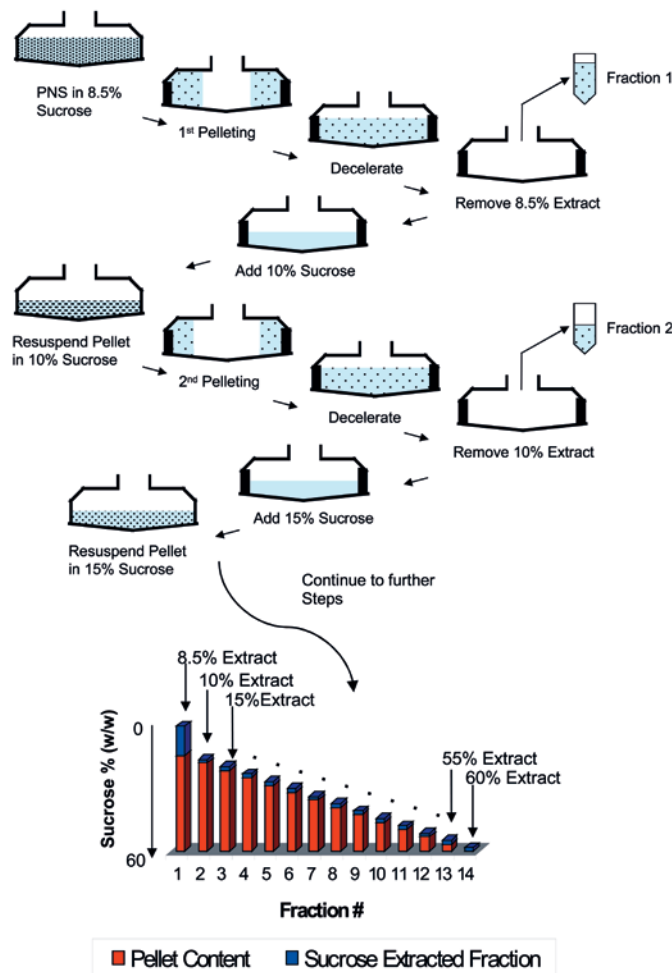


FIGURE 1

PNS of rat livers and brains was fractionated using the Edge 200 Separation System. The step-wise density gradient extraction process is described as follows: 3 mL of PNS in 250 mM (~8.5%) sucrose was loaded in a rotor sample container; the rotor sample container in a rotor was spun for 30 min to pellet all the subcellular particles except soluble proteins and very small particles. The supernatant was removed. The pellet was resuspended in 10% sucrose solution and spun for 2 min. After the supernatant was removed, the pellet was resuspended in 15% sucrose solution and spun for 2 min. The process was continued in the same manner through the last fraction, which was 60% sucrose. The speed of the rotor was 95K rpm with an average 120K g force.

mass spectrometry, and microarray. The following steps describe how the technology works:

1. Suspending the particles in an initial medium of known density (d_1).
2. Letting the d_1 suspension settle, or pelleting to enhance settling through centrifugation.
3. Collecting those particles remaining suspended in the d_1 supernatant.
4. Resuspending the resultant pellet in an extracting medium of a greater density (d_2) than that of the initial medium.
5. Letting the d_2 suspension settle, or pelleting to enhance settling through centrifugation.
6. Repeating the above process as desired.

Thus, since density d_2 is greater than density d_1 , the particles extracted in the d_2 supernatant will necessarily have a density greater than d_1 but less than or equal to d_2 . Essentially, the particles obtained in this manner will have a net buoyancy in the extracting medium. Figure 1 shows the work flow of Edge technology schematically.

Edge technology not only reduces sample complexity significantly, but also provides many benefits that traditional methods will not achieve. Due to the stepwise extraction process, extraction may start at any density step of interest, without the need for going through the whole gradient. The method does not require a density gradient medium and does not require a gradient mixer. In addition, the density of the extraction medium at each step is pre-defined, and no other instrument is needed for density determination. Furthermore, the user has the flexibility to control the separation resolution and extraction volume. The starting material stays in the same sample container for the whole fractionation process; thus, high recovery yields can be obtained.

The Edge 200 Separation System is an easy to use, bench-top air-driven ultracentrifuge system (Figure 2). It can reach 95,000 to 100,000 rpm within a minute and provide 120,000 to 150,000 g. The separation system provides defined, non-denaturing, and reproducible fractionation of complex biological samples by their densities.



FIGURE 2

Edge 200 Separation System with sample rotor and rotor sample container.

In this study, we used Edge 200 Separation System and fractionated rat livers and brains. Tables 1 and 2 show the protein concentrations of those fractions from livers and brains of three control rats and three FD rats.

Western Blot Analysis

GPx-1 is a protein involved in the control of oxidative stress; GRP75 is known as mitochondrial heat shock protein 70 (HSP70).³⁹ We used these two markers in western blot analysis to investigate folate deficiency and the resulting differential expression levels of these markers in both liver and brain in the same animal. Initially, in order to verify the literature results, we performed western analysis on liver and brain PNS from control and FD rats, i.e., the materials before fractionation (Figures 3 and 4). In the liver PNS, GPx1 was increased in abundance about 50 to 70% in FD rats. In contrast to GPx1, GRP75

decreased in abundance about 20–30% in FD rats. This is consistent with the previous literature report.³⁴ It also was known that folate deficiency would elevate plasma homocysteine levels, increase rat liver lipid peroxidation, and induce oxidative stress in rat liver.³⁸ However, more data are still needed to determine whether mild hyperhomocysteinemia or oxidative stress in FD rats caused down-regulation of GRP75. On the other hand, both GPX1 and GRP75 in brain PNS were observed in slightly higher expression in FD rats (Figure 4). This was again in line with previous reports that dietary folate deficiency in mice would increase GPX expression level in brain tissue.²⁶ However, GRP75 expression level changes in brain tissue in FD rats have not been reported before. Overall, this preliminary study showed that FD-induced oxidative stress occurred more in rat liver tissue than in rat brain tissue. Whether this result can be correlated with a previous report, in which folate concentrations in rats fed with folate deficiency diet were 60% lower in liver but were the same in brain,³⁵ is unknown at this time.

The western blot analysis results of both liver and brain PNS in FD rats not only were consistent with previous studies but also demonstrated the different responses to folate deficiency between the two tissues in the same animal. However, in order to discover the oxidative stress induced by folate deficiency at subcellular levels, western blot analysis was performed on all fractions from both liver and brain obtained by the Edge 200 Separation System. In the traditional western blot analysis, the global expression of each marker in FD rats was measured and

TABLE 1

Protein Concentrations of Fractionated Rat Livers and Brains

Fr #	CONTROL						FD					
	RAT #1		RAT #2		RAT #3		RAT #4		RAT #5		RAT #6	
	Brain	Liver	Brain	Liver	Brain	Liver	Brain	Liver	Brain	Liver	Brain	Liver
PNS	11.02	14.52	13.97	16.27	12.34	16.30	11.56	16.69	13.04	13.31	12.00	13.38
10%	1.86	2.85	1.77	2.11	0.84	2.87	1.88	2.37	1.35	2.13	1.91	1.96
15%	1.07	1.38	1.30	1.58	1.34	2.14	1.32	1.45	1.04	1.22	1.34	1.54
20%	0.97	1.31	1.35	1.52	1.75	1.88	1.24	1.1	0.95	0.99	1.44	1.34
25%	1.96	1.17	2.14	1.59	1.97	2.61	1.54	1.14	1.81	0.87	2.04	1.21
30%	1.73	1.12	3.25	3.11	3.24	4.56	2.4	1.51	2.91	1.43	3.03	1.98
35%	4.03	2.75	5.07	4.08	4.46	4.72	4.52	3.26	4.58	3.76	4.44	4.16
40%	2.88	2.25	3.67	2.81	3.72	3.72	3.12	2.95	4.10	4.16	3.74	3.86
45%	1.00	1.05	0.93	1.47	0.69	2.39	0.86	1.40	0.95	3.00	0.62	2.58
50%	0.44	0.48	0.47	0.45	0.45	0.63	0.54	0.37	0.36	0.69	0.24	0.63
55%	0.31	—	0.35	0.16	0.38	0.33	0.42	0.19	0.30	0.47	0.30	0.36
60%	0.37	—	0.40	0.19	0.51	0.23	0.41	0.15	0.38	0.38	0.37	0.37

Summary of protein concentrations of all fractions from both livers and brains including PNS from both tissues. The protein concentrations were determined by BCA assay in mg/mL.

TABLE 2

Protein ID of Selected Spots Using MALDI-TOF/TOF

	Spot	Protein	Accession #	Protein Score	Total Ion Score	Relative Expression
Fr 30%	0012	similar to NADH dehydrogenase:Ubiquinone Fe-S protein 8	gi 27661165	339	286	Down
	4305	NADH dehydrogenase (ubiquinone) 1 alpha subcomplex 10	gi 46391108	498	410	Down
	3305	fructose-1,6-biphosphatase 1	gi 51036635	568	435	Unique to Control
	5001	Calreticulin	gi 11693172	772	718	Unique to Control
	0201	Annexin A5	gi 51858950	851	726	Unique to FD
	3607	similar to alpha-1 major acute phase protein prepeptide	gi 57526868	835	690	Up
Fr 40%	1202	regucalcin	gi 13928740	178	136	Down
	2214	estrogen sulfotransferase iso-mer 3	gi 2144059	202	123	Down
	4008	chain D, rat transthyretin	gi 3212535	289	222	Down
	4505	4-trimethylaminobutyraldehyde dehydrogenase	gi 7248632	464	353	Unique to Control
	8507	similar to 6-phosphogluconate dehydrogenase,decarboxylating	gi 33086672	268	241	Unique to Control
	9611	fibrinogen, beta polypeptide	gi 56971493	684	534	Unique to FD
	3702	Hpx protein	gi 60688311	472	382	UP
	2411	unknown	gi 44890246	112	37	UP
8208	haptoglobin	gi 59808182	483	395	UP	

Selected 2D gel spots were subjected to in-gel tryptic digestion. Digested samples were spotted on MALDI plate, and the protein identification was performed by searching the combined MS and MS/MS spectra against the SwissProt database as described in Materials and Methods.

compared with the global expression of the marker in control rats (Figures 3 and 4). In this study, we have examined the relative percentage distribution of each marker by fraction for each animal. Figures 5 and 6 show the western analysis of GPx1 and GRP 75 from the rat-liver fractions. There were significant differences of the relative percentage distributions between control and FD rats for both markers. In the western blot analysis of GPx1 from rat liver, a down-regulation of greater than twofold in FD rats was observed in the 30% sucrose fraction, and an up-regulation of greater than twofold in FD rats was found in the 40% sucrose fraction (Figure 5). In GRP75 western blot analysis of rat liver, results were similar to those observed with GPx1, but with a slight difference. More than twofold down-regulation of GRP75 in FD rats was detected in the 30% sucrose fraction, and more than twofold up-regulation of the marker in FD rats was found in the 45% sucrose fraction (Figure 6).

In the western blot analysis of fractionated brain tissues, both markers were shown in highest abundance in the 35% and 40% sucrose fractions (Figures 7 and 8).

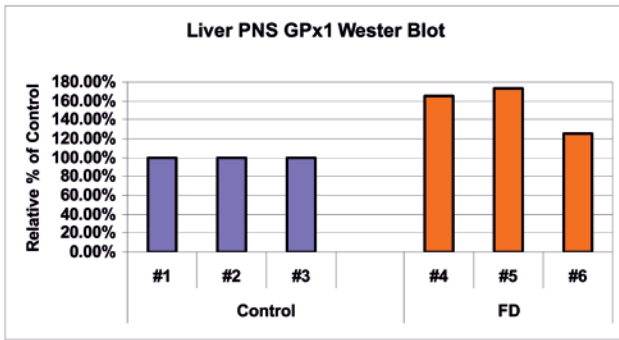
However, there was little change of relative percentage distribution for both markers (<25%) between control and FD rats across all fractions, which mirrors the western blot results of brain PNS, showing a similar degree of regulation of both markers in FD rats. Therefore, oxidative stress induced by folate deficiency, as indicated by measurement of GPx1 and GRP75, is less in brain tissue than in liver tissue.

These western blot results demonstrated that the density-based fractionation revealed much bigger changes (> twofold) in certain liver fractions in FD rats compared with the traditional western blot analysis without fractionation. This data provide new insights into the relative differential expression levels of the markers in different density fractions, which may relate to different subcellular compartments.

2D Gel Analysis and Mass Spectrometric Protein Identification

The western analysis results above showed that the biggest relative percentage distribution changes in both markers

Western Blot Analysis of Liver PNS



A

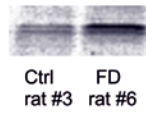
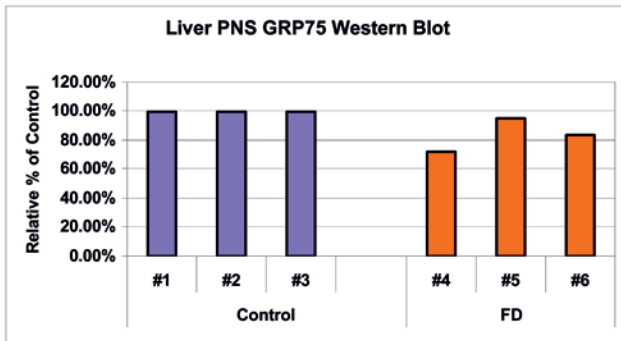


FIGURE 3

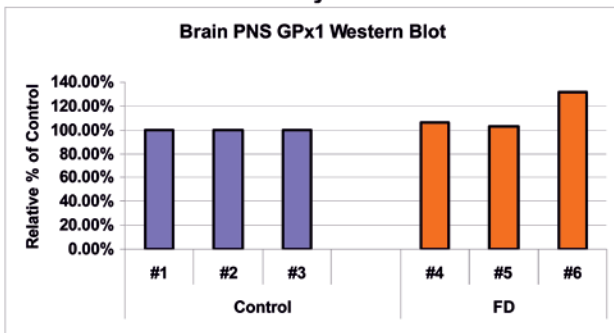
Western blot analysis of rat liver PNS from control and FD rats before fractionation. Equal amount of total protein was subjected to western analysis as described under Materials and Methods. **A:** Relative expressions of GPx1 of liver PNS in three control and three FD rats. **B:** Relative expressions of GRP75 of liver PNS in three control and three FD rats.



B



Western Blot Analysis of Brain PNS



A

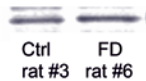
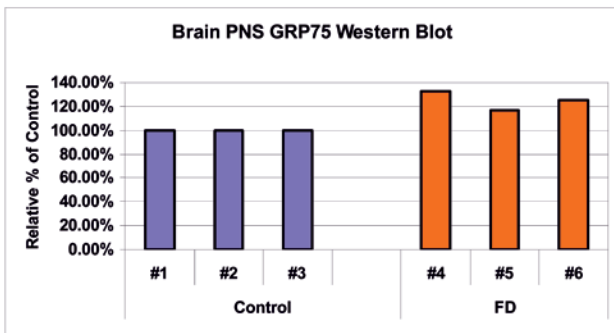
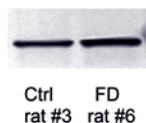


FIGURE 4

Western blot analysis of rat brain PNS from control and FD rats before fractionation. Equal amount of total protein was subjected to western analysis as described under Materials and Methods. **A:** Relative expressions of GPx1 of brain PNS in three control and three FD rats. **B:** Relative expressions of GRP75 of brain PNS in three control and three FD rats.



B



Western Blot Analysis of Liver GPx1

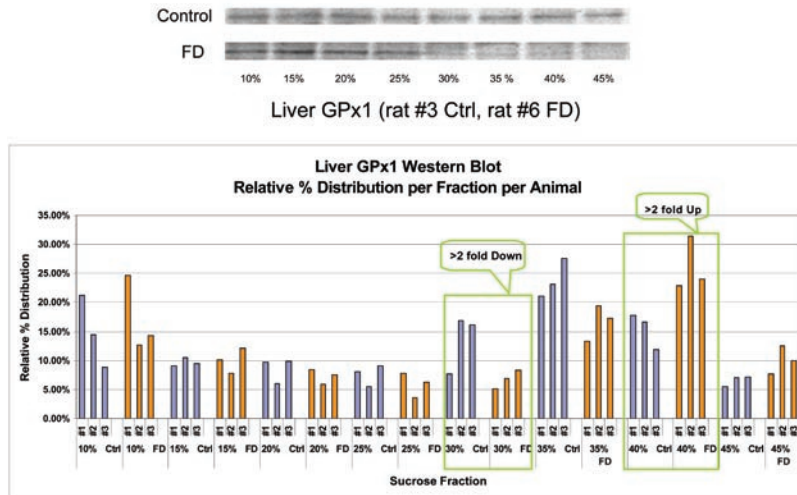


FIGURE 5

Western blot analysis of GPx1 of fractionated liver from control and FD rats. Relative percentage distribution of each fraction was calculated from the intensity of immuno-signal from each fraction divided by the sum of intensity of all fractions. The western blot images from rat #3 (Ctrl) and rat #6 (FD) are shown.

between control and FD rat liver tissue were observed in 30% and 40% sucrose fractions. In order to correlate the biological information from these results, protein profiles as well as the relative protein abundance levels were investigated using 2DE and MALDI-TOF/TOF.

The two fractions from liver (30% and 40%) of individual animals from both groups (control #3 and FD #6), were selected for 2D gel analysis. The 2D gels from the selected fractions were done in duplicate with the same amount of total protein loaded per gel. The gels were stained with coomassie blue and then digitized for image analysis. Figure 9 shows the selected areas of 2D gel image results from the 2 liver fractions using the PDQuest software. The images show expanded regions surrounding interesting spots. Under these experimental conditions,

172 spots were shown to have a volume change of more than twofold compared with the control rat in the liver 30% sucrose fraction, while 192 spots, separated with the same criteria, were identified in the liver 40% sucrose fraction. After evaluating those spots manually, 6 spots from the 30% sucrose fraction and 10 spots from the 40% sucrose fraction were subjected to in-gel digestion and MALDI-TOF/TOF analysis. Table 2 summarizes all the proteins identified from the selected spots from both liver fractions meeting the database search criteria, as described in the Materials and Methods section. Among those identified proteins, there are several unknown or theoretical proteins, whose DNA sequences were known or predicted only by computational methods. Figures 10 and 11 show the MALDI MS and MS/MS spectra of two theoretical

Western Blot Analysis of Liver GRP75

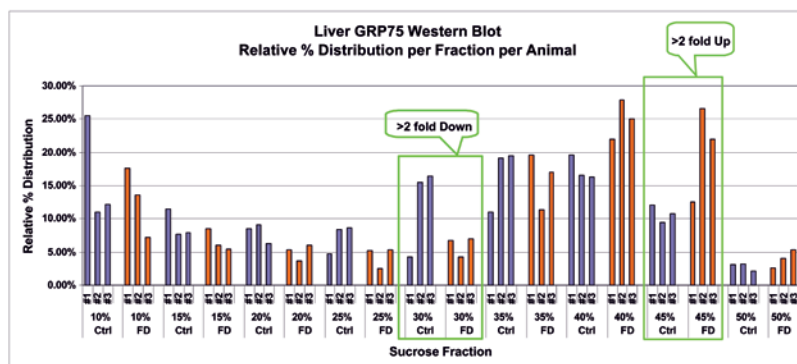
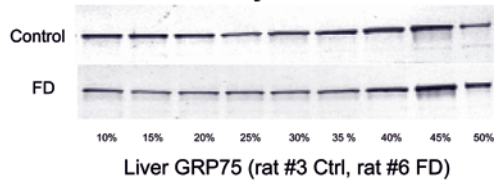
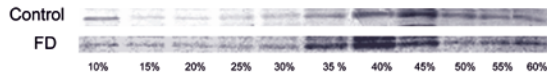


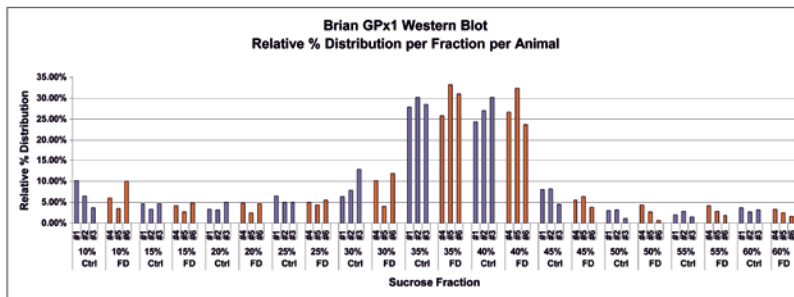
FIGURE 6

Western blot analysis of GRP75 of fractionated liver from control and FD rats. Relative percentage distribution of each fraction was calculated from the intensity of immuno-signal from each fraction divided by the sum of intensity of all fractions. The western blot images from rat #3 (Ctrl) and rat #6 (FD) are shown.

Western Blot Analysis of Brain GPx1



Brain GPx1 (rat #2 Ctrl, rat #5 FD)

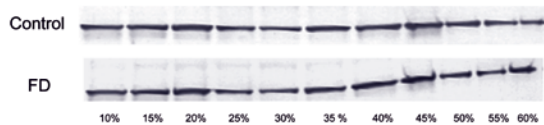


proteins, (a) similar to 6-phosphogluconate dehydrogenase, decarboxylating, and (b) similar to alpha-1 major acute-phase protein prepeptide, identified in rat liver 40% and 30% sucrose fractions, respectively. These unknown proteins could play important roles in understanding the relationship of folate deficiency and oxidative stress. Additionally, most of the other known proteins identified as showing significant regulation changes in these two fractions are oxidative stress related (Table 2). For example, NADH dehydrogenase (ubiquinone) 1 alpha subcomplex 10 was found to be significantly down-regulated in the FD rat liver 30% sucrose fraction. This protein is part of mitochondrial complex I, which plays a key role in cellular metabolic processes and affects normal mitochondrial physiology. Recent reports have demonstrated oxidative stress will inhibit mitochondrial NADH dehydrogenase activity and lead to many mitochondrial diseases and neurological disorders.^{40–42} Calreticulin, an endoplasmic reticulum (ER) calcium-binding protein, was present in

the control rat but was not detected in the FD rat liver 30% sucrose fraction. This finding was consistent with several previous studies showing that oxidative stress would decrease calreticulin expression level and inhibit ER protein processing and cellular protein synthesis.^{43–45} This protein, however, could be translocated to another fraction. Annexin 5 was detected only in the FD rat liver 30% sucrose fraction. Annexin A5 is one of the family of calcium- and phospholipid-binding proteins that are involved in membrane fusion and signal transduction.⁴⁶

In the list of proteins identified from the liver 40% sucrose fraction, the expression of regucalcin is significantly lower in FD rats, while fibrinogen was detected only in FD rat. Both proteins are involved in blood clotting, oxidative stress, electron transport, and calcium regulation.⁴⁷ Rat transthyretin, observed as down-regulated in the FD rat liver 40% sucrose fraction, was reported to play an important role in triggering inflammatory and oxidative stress pathways.⁴⁹ Another down-regulated protein

Western Blot Analysis of Brain GRP75



Brain GRP75 (rat #2 Ctrl, rat #5 FD)

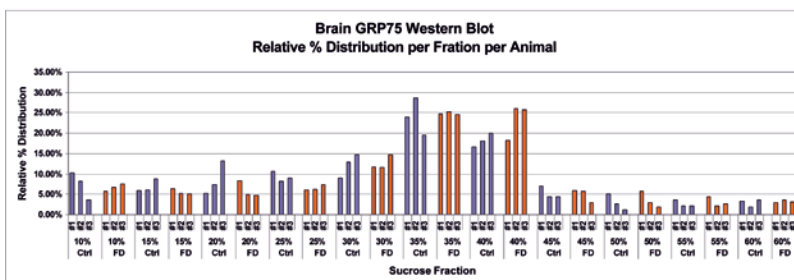


FIGURE 7

Western blot analysis of GPx1 of fractionated brain from control and FD rats. Relative percentage distribution of each fraction was calculated from the intensity of immuno-signal from each fraction divided by the sum of intensity of all fractions. The western blot images from rat #2 (Ctrl) and rat #5 (FD) are shown.

FIGURE 8

Western blot analysis of GRP75 of fractionated brain from control and FD rats. Relative percentage distribution of each fraction was calculated from the intensity of immuno-signal from each fraction divided by the sum of intensity of all fractions. The western blot images from rat #2 (Ctrl) and rat #5 (FD) are shown.

**2D Gel Images of Selected Liver Fractions
(Animals #3 and #6)**

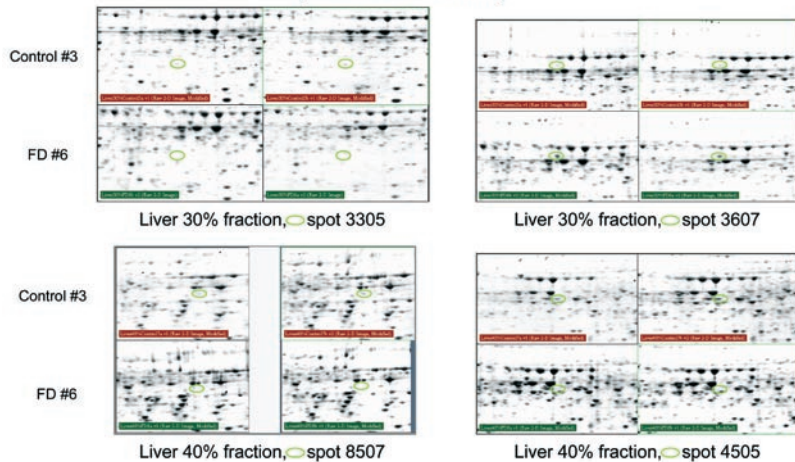


FIGURE 9

Details of 2D gel images of liver fractions 30% and 40%, showing selected differentially regulated proteins. Fractions from control rat #3 and FD rat #6 were selected for 2D gel analysis as described under Materials and Methods.

in this fraction, estrogen sulfotransferase, is a well known liver-specific enzyme that catalyzes the sulfoconjugation and inactivation of estrogens.⁴⁸ Whether this protein is related to folate deficiency-induced oxidative stress is still unknown. 4-Trimethylaminobutyraldehyde dehydrogenase functions in carnitine biosynthesis, and it catalyzes the oxidation of 4-N-trimethylaminobutyraldehyde to form 4-trimethylaminobutyrate.⁵⁰ Among the two known up-regulated proteins in the FD rat liver 40% sucrose fraction, Hpx is a plasma protein with the highest binding affinity to heme among known proteins and acts as an

antioxidant after blood heme overload,⁵¹ while haptoglobin is mainly produced in the liver, and its major biological function involves preventing the hemoglobin-driven generation of hydroxyl radicals and lipid peroxides.^{52,53}

On the other hand, 2D gel analysis of the 40% sucrose fraction of rat brain showed very little change. Figure 12 shows the overlay of the 2D gels of control and FD rat fraction 40%. Although the image analysis found 80 spots with their volume changes more than twofold in FD rats, there was no spot showing significant changes after verifying those spots manually. More fractions in FD rat brain

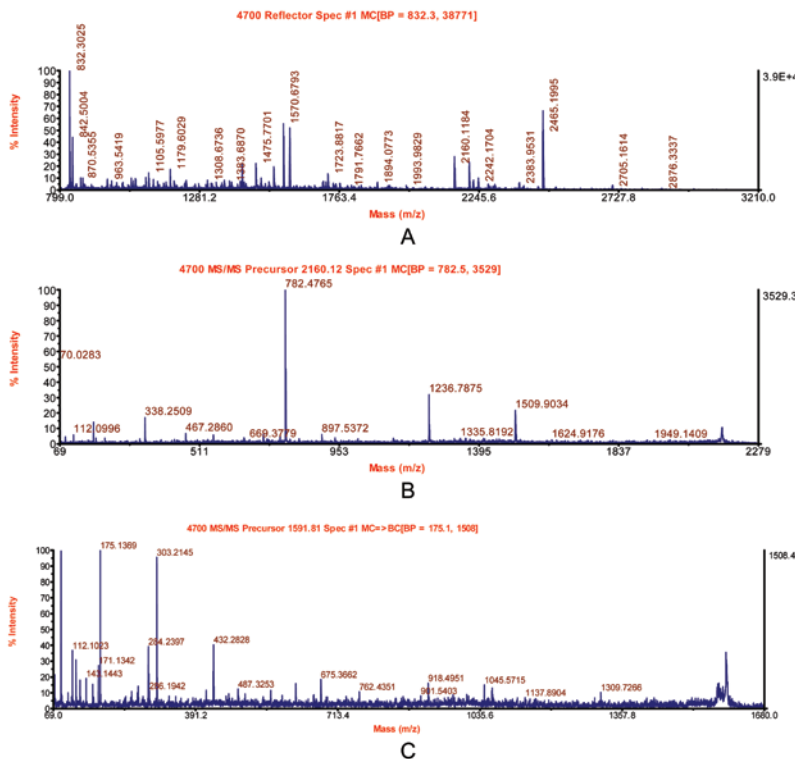


FIGURE 10

MALDI-TOF/TOF spectra of protein “similar to similar to 6-phosphobluconate dehydrogenase, decarboxylating,” identified from 2D gel spot number 8507 of rat liver 40% sucrose fraction. **A:** Total ion scan. **B:** MS/MS spectrum of the precursor 1591.81. **C:** MS/MS spectrum of the precursor 2160.12.

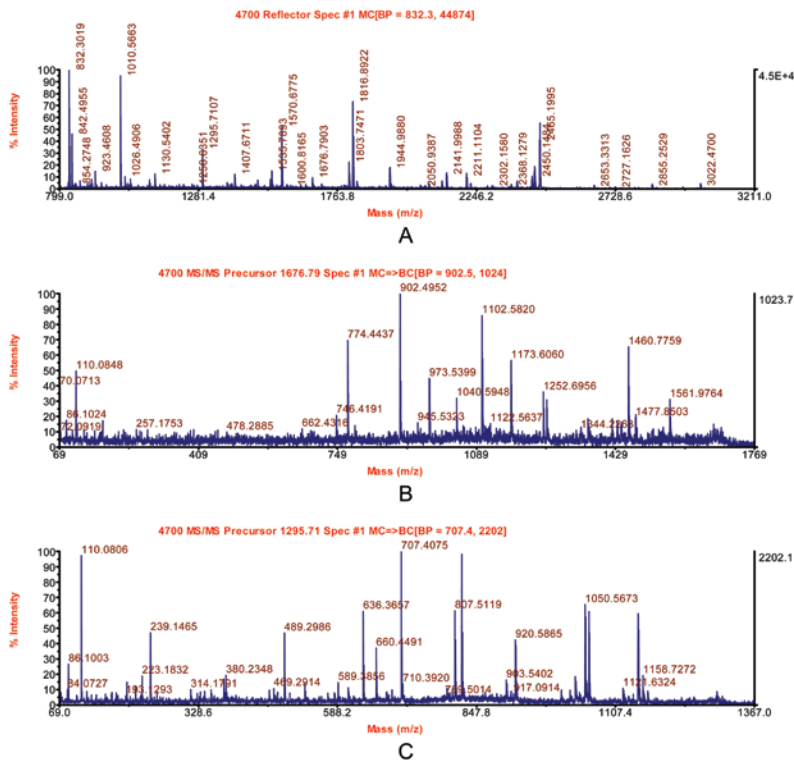


FIGURE 11

MALDI-TOF/TOF spectra of protein “similar to alpha-1 major acute phase protein prepeptide,” identified from 2D gel spot number 3607 of rat liver 30% sucrose fraction. **A:** Total ion scan. **B:** MS/MS spectrum of the precursor 1295.71. **C:** MS/MS spectrum of the precursor 1676.79.

need to be evaluated by 2DE before drawing any conclusions about whether folate deficiency affects regulation levels in the protein profiles in brain tissue.

Protein identification data presented above represent only a small number of selected spots from two fractions of the total separation. It is thus expected that a significantly larger database can be generated.

CONCLUSIONS

Western blot results show changes in the relative percentage distribution of markers per fraction, indicating their

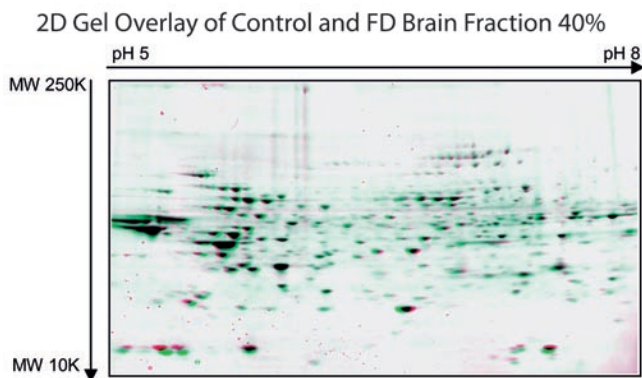


FIGURE 12

2D gel images overlay of control and FD rat brain fraction 40%. The overlay image was performed by the PDQuest software. Control rat #3 and FD rat #6 were selected for 2D gel analysis, as described under Materials and Methods.

potential translocation in the cell. Rat liver appears to show a much higher response to folate deficiency than does rat brain, with little or no correlation between organs. Further investigation is needed to explore the biological roles of those identified proteins, especially those unique and theoretical proteins, found by MALDI-TOF/TOF, that could be potential biomarkers for folate deficiency.

Edge technology provides a rapid screening method for various biomarkers by enriching those markers in defined fractions. This fractionation method provides a powerful tool to see the significant differences between treated and control groups, as well as assessing inter-animal variation within the three FD and three control animals. Furthermore, since the fractionation method separated complex samples as individual compartments, most of the functional and low-abundance proteins inside the compartments were preserved, retaining biological information that is easily lost using other sample-preparation methods.

REFERENCES

- Ghoshal K, Li X, Datta J, Bai S, Pogribny I, Pogribny M, et al. A folate- and methyl-deficient diet alters the expression on DNA methyltransferases and methyl CpG binding proteins involved in epigenetic gene silencing in livers of F344 rats. *J Nutri* 2006;136:1522–1527.
- Mattson MP, Shea TB. Folate and homocysteine metabolism in neural plasticity and neurodegenerative disorders. *Trends Neurosci.* 2003;26(3):137–146.

3. Clarke R, Smith AD, Jobst KA, Refsum H, Sutton L, Ueland PM. Folate, vitamin B12, and serum total homocysteine levels in confirmed Alzheimer's disease. *Arch Neurol* 1998;55:1449–1455.
4. Ebly EM, Schaefer JP, Campbell NR, Hogan DB. Folate status, vascular disease, and cognition in elderly Canadians. *Age Aging* 1998;27:485–491.
5. Hassing L, Wahlin A, Winblad B, Bäckman L. Further evidence on the effects of vitamin B12 and folate levels on episodic memory functioning: A population-based study of healthy very old adults. *Biol Psych* 1999;45:1472–1480.
6. Wang HX, Wahlin A, Basun H, Fastbom J, Winblad B, Fratiglioni L. Vitamin B12 and folate in relation to the Alzheimer's disease. *Neurology* 2001;56:1188–1194.
7. Gray, GE. Nutrition and dementia. *J Am Diet Assoc* 1989;89:1795–1802.
8. Duan W, Ladenheim B, Cutler RG, Kruman II, Cadet JL, Mattson MP. Dietary folate deficiency and elevated homocysteine levels endanger dopaminergic neurons in models of Parkinson's disease. *J Neurochem* 2002;80:101–110.
9. Choi SW, Mason JB. Folate and carcinogenesis: An integrated scheme. *J Nutr* 2000;130:129–132.
10. Verhaar MC, Strose E, Rabelink TJ. Foliates and cardiovascular diseases. *Arterioscler Thromb Vasc Biol* 2002;22(1):6–13.
11. Poirier LA, Wise CK, Delongchamp RR, Sinha R. Blood determinations of S-adenosylmethionine, S-adenosylhomocysteine, and homocysteine: correlation with diet. *Cancer Epidemiol Biomarkers Prev* 2001;10:649–655.
12. Duthie SJ, Narayanan S, Sharp L, Little J, Basten G, Powers H. Folate, DNA stability and colo-rectal neoplasia. *Proc Nutr Soc* 2004;63:571–578.
13. James SJ, Pogribny IP, Pogribna M, Miller BJ, Jernigan S, Melnyk S. Mechanisms of DNA damage, DNA hypomethylation, and tumor progression in the folate/methyl-deficient rat model of hepatocarcinogenesis. *J Nutr* 2003;133 (11 suppl 1):3740S–3747S.
14. Giovannucci E, Rimm EB, Ascherio A, Stampfer MJ, Colditz GA, Willett WC. Alcohol, low-methionine–low-folate diets, and risk of colon cancer in men. *J Natl Cancer Inst* 1995;87:265–273.
15. Crott JW, Mashiyama ST, Ames BN, Fenech M. The effect of folic acid deficiency and MTHFR C677T polymorphism on chromosome damage in human lymphocyte in vitro. *Cancer Epidemiol Biomarkers Prev* 2001;10:1089–1096.
16. Mattson MP, Shea TB. Folate and homocysteine metabolism in neural plasticity and neurodegenerative disorders. *Trends Neurosci* 2003;26(3):137–146.
17. Ho PI, Ortiz D, Rogers E, Shea TB. Multiple aspects of homocysteine neurotoxicity: Glutamate excitotoxicity, kinase hyperactivation and DNA damage. *J Neurosci Res* 2002;70:694–702.
18. Kruman II, Culmsee C, Chan SL, Kruman Y, Guo Z, Penix L, et al. Homocysteine elicits a DNA damage response in neurons that promotes apoptosis and hypersensitivity to excitotoxicity. *J Neurosci* 2000;20(18):6920–6926.
19. Aksenov M, Aksenova M, Butterfield DA, Markesbery WR. Oxidative modification of creatine kinase BB in Alzheimer's disease brain. *J Neurochem* 2000;74:2520–2527.
20. Castegna A, Aksenov M, Thongboonkerd V, Klein JB, Pierce WM, Booze R, et al. A proteomics identification of oxidatively modified proteins in Alzheimer's disease brain: Part II: Dihydropyrimidinase-related protein 2, alpha-enolase and heat shock cognate. *J Neurochem* 2002;82:1524–1532.
21. Castegna A, Aksenov M, Aksenova M, Thongboonkerd V, Klein JB, Pierce WM. A proteomics identification of oxidatively modified proteins in Alzheimer's disease brain: Part I: Creatine kinase BB, glutamine synthase, and ubiquitin carboxy-terminal hydrolase L-1. *Free Radic Biol Med* 2000;33:562–571.
22. Uthus EO, Ross SA, Davis CD. Differential effects of dietary selenium (se) and folate on methyl metabolism in liver and colon of rats. *Biol Trace Elem Res* 2006;109(3):201–214.
23. Brunaud L, Alberto JM, Ayav A, Gerard P, Namour F, Antunes L. Effects of vitamin B12 and folate deficiencies on DNA methylation and carcinogenesis in rat liver. *Clin Chem Lab Med* 2003;41(8):1012–1019.
24. Ghandour H, Lin BF, Choi SW, Mason JB, Selhub J. Folate status and age affect the accumulation of l-isoaspartyl residues in rat liver proteins. *J Nutr* 2002;132(6):1357–1360.
25. Crott JW, Choi SW, Branda RF, Mason JB. Accumulation of mitochondrial DNA deletions is age, tissue and folate-dependent in rats. *Mutation Res* 2005;570:63–70.
26. Shea TB, Rogers E, Ashline D, Ortiz D, Sheu MS. Apolipoprotein E deficiency promotes increased oxidative stress and compensatory increase in antioxidants in brain tissue. *Free Radic Biol Med* 2002;33(8):1115–1120.
27. Kinoshita Y, Uo T, Jayadev S, Garden GA, Conrads TP, Veenstra TD, et al. Potential applications and limitations of proteomics in the study of neurological disease. *Arch Neurol* 2006;63(12):1692–1696.
28. Pierce JD, Fakhari M, Works KV, Pierce JT, Clancy RL. Understanding proteomics. *Nurs Health Sci* 2007;9(1):54–60.
29. Chuthapishith S, Layfield R, Kerr ID, Eremin O. Principles of proteomics and its application in cancer. *Surgeon* 2007;5(1):14–22.
30. Wang Y, Chiu JF, He QY. Proteomics approach to illustrate drug action mechanisms. *Curr Drug Discov Technol* 2006;3(3):199–209.
31. Matt P, Carrel T, White M, Lefkovits I, Van Eyk J. Proteomics in cardiovascular surgery. *J Thorac Cardiovasc Surg* 2007;133(1):210–214.
32. Kussmann M, Raymand F, Affolter M. OMICS-driven biomarker discovery in nutrition and health. *J Biotechnol* 2006;124(4):758–787.
33. Kussmann M. How to comprehensively analyze proteins and how this influences nutritional research. *Clin Chem Lab Med* 2007;45(3):288–300.
34. Chanson A, Sayd T, Rock E, Chambon C, Santé-Lhoutellier V, Potier de Courcy G, et al. Proteomic analysis reveals changes in the liver protein pattern of rats exposed to dietary folate deficiency. *J Nutr* 2005;135(11):2524–2529.
35. Varela-Moreiras G, Selhub J. Long-term folate deficiency alters folate content and distribution differentially in rat tissues. *J Nutr* 1992;122:986–991.
36. Balaghi M, Horne DW, Wagner C. Hepatic one-carbon metabolism in early folate deficiency in rats. *Biochem J* 1993;291(Pt 1):145–149.
37. Mato JM, Lu SC. Homocysteine, the bad thio. *Hepatology* 2005;41(5):976–979.
38. Huang RF, Hsu YC, Lin HL, Yang FL. Folate depletion and elevated plasma homocysteine promote oxidative stress in rat livers. *J Nutr* 2001;131:33–38.
39. Webster TJ, Naylor DJ, Hartman DJ, Hoj PB, Hoogenraad NJ. cDNA cloning and efficient mitochondrial import of pre-mtHSP70 from rat liver. *DNA Cell Biol* 1994;13(12):1213–1220.
40. Schapira AH, Cooper JM, Dexter D, Clark JB, Jenner P, Marsden CD. Mitochondrial complex I deficiency in Parkinson's disease. *J Neurochem* 1990;54:823–827.
41. Lenaz G, Bovina C, D'Aurelio M, Fato R, Formiggini G, Genova ML, et al. Role of mitochondria in oxidative stress and aging. *Ann NY Acad Sci* 2002;(959):199–213.
42. Schilling B, Bharath MMS, Row RH, Murray J, Cusack MP, Capaldi RA, et al. Rapid purification and mass spectrometric characterization of mitochondrial NADH dehydrogenase (complex I) from rodent brain and a dopaminergic neuronal cell line. *Mol Cell Proteomics* 2005;4(1):84–96.
43. Liu H, Bowes RC 3rd, van de Water B, Silience C, Nagelkerke JF, Stevens JL. Endoplasmic reticulum chaperones GRP78 and calreticulin prevent oxidative stress, Ca²⁺ disturbances, and cell death in renal epithelial cells. *J Biol Chem* 1997;272(35):21751–21759.
44. Dreher D, Vargas JR, Hochstrasser DF, Junod AF. Effects of oxidative stress and Ca²⁺ agonists on molecular chaper-

- ones in human umbilical vein endothelial cells. *Electrophoresis* 1995;16:1205–1214.
45. Rabek JP, Boylston WH III, Papaconstantinou J. Carbonylation of ER chaperone protein in aged mouse liver. *Biochem Biophys Res Comm* 2003;305:566–572.
46. Hu R, Jin H, Zhou S, Yang P, Li X. Proteomic analysis of hypoxia-induced responses in the syncytialization of human placental cell line BeWo. *Placenta* 2007;28(5–6):399–407.
47. Bruggeman V, Van den Bergh G, Clerens S, Dumez L, Onagbesan O, Arckens L, et al. Effect of a single *in ovo* injection of 2,3,7,8-tetrachlorodibenzo-p-dioxin on protein expression in liver and ovary of the one-day-old chick analyzed by fluorescent two-dimensional difference gel electrophoresis and mass spectrometry. *Proteomics* 2006;6(8):2576–2585.
48. Song WC. Biochemistry and reproductive endocrinology of estrogen sulfotransferase. *Ann NY Acad Sci* 2002;948:43–50.
49. Saraiva MJ. Cellular consequences of transthyretin deposition. *Amyloid* 2003;10 (Suppl 1):13–16.
50. Hulse JD, Henderson LM. Carnitine biosynthesis. *J Biol Chem* 1980;255(3):1146–1151.
51. Tolosano E, Altruda F. Hemopexin: Structure, function, and regulation. *DNA Cell Bio* 2002;21(4):297–306.
52. Gutteridge JM. The antioxidant activity of haptoglobin towards haemoglobin-stimulated lipid peroxidation. *Biochim Biophys Acta* 1987;917:219–223.
53. Lim SK, Ferraro B, Moore K, Halliwell B. Role of haptoglobin in free hemoglobin metabolism. *Redox Report* 2001;6:219–227.